

## THE INFLUENCE OF CARBIDE DISTRIBUTION ON TEXTURE FORMATION IN A FAST ANNEALED A $\delta$ -KILLED STEEL

C.S. DA COSTA VIANA, L.P.M. BRANDÃO and  
I.O. DE MEDEIROS  
IME-SE/4 - BRASIL

### INTRODUCTION

It is well known that the forming behaviour of sheet metals is directly related to their crystallographic textures. In Steels, a near ideal texture for a good performance in deep drawing operations can be described by the strong fiber components  $\{111\} \langle uvw \rangle$  and  $\{hk\ell\} \langle 110 \rangle$  which maximize the R-values. Traditionally, the best behaviour in carbon steels is obtained for box-annealed 70% cold rolled material<sup>1, 2</sup>. Besides being discontinuous, box-annealing is a very time-consuming treatment, this fact having contributed to the development of the continuous annealing process. However, the high heating and cooling rates of the latter does not allow an adequate texture control via aluminium nitride precipitation, as in box-annealing, giving rise to weak textured materials. Also, microstructural features were found to affect texture development in this process making it difficult to obtain high R-values in the final material<sup>3, 4</sup>. In this respect, some workers have concluded that the presence of carbon in solid solution or as fine precipitates hinder the development of the  $\{111\} \langle uvw \rangle$  fiber components both in the cold rolling and the recrystallization textures<sup>3-6</sup>. It is accepted that fine carbides are more detrimental than coarse ones<sup>5</sup>. Hutchinson<sup>3, 4</sup> suggested that better texture can be obtained in steels with fewer and coarser cementite particles. Recently, Magnabosco<sup>7</sup> obtained strong  $\{111\} \langle uvn \rangle$  components in a solution treated steel sheet.

Annealing textures are influenced by many processing variables: coiling and annealing temperatures, heating and cooling rates, cold rolling reduction, among others. It is also dependant on the cold rolling texture. In particular, this is affected by the presence of hard particles in the matrix, as demonstrated by Dillamore et al.<sup>6</sup>, leading to a

degradation of forming properties, as verified by Hosford and Zeisloft<sup>8</sup>.

In the present work an attempt is made to correlate the presence of carbon both in solid solution and as precipitates with the cold rolling and annealing textures of a low carbon Al-killed steel.

#### **EXPERIMENTAL PROCEDURE**

Commercial Al-killed steel for deep drawing operations coiled at 903K (630°C) was used. Its chemical composition is shown in table I. The material was received as hot rolled band with a thickness of 2.7 mm.

Most of the hot rolled material was soaked at 973K (700°C) for 30 minutes, in a salt bath, and quenched to room temperature (25°C) in brine. This ensured little alteration of the grain structure while dissolving about 50% of the cementite and precipitating most of the AlN.

Part of the quenched material was aged at different temperatures and time periods: 473K (200°C) for 20 minutes, 673K (400°C) for 10 minutes and 873K (600°C) for 7 minutes. The time periods corresponded to the hardness peaks determined in previous ageing treatments. The idea was to obtain the largest influence possible of the precipitated particles on plastic flow and thus alter the crystal rotations and the rolling texture as a consequence.

All specimens were 80% cold rolled in light passes and with liquid cooling, to avoid altering the initial treatments, and annealed at 1123K (850°C) for 5 minutes, in a salt bath, immediately after. Specimen identification used the notation: AR - as received, S - solution heat treated, SAX - aged at X(0,2,4 or 6) where X stands for the ageing temperatures 200°C, 400°C or 600°C, respectively.

The texture was quantified by the crystallite orientation distribution function (CODF) using the method of incomplete pole figures developed by Morris. Three pole distributions were used and the series coefficients were calculated to the order of  $l = 20$ . No zero-order correction was used. The CODF sections were drawn in times random units, the dotted line corresponding to 1 and the others to increments of 1.

## RESULTS

The as-received material showed a ferritic microstructure with a grain size of  $8.3\mu\text{m}$  and few colonies of pearlite. This microstructure did not undergo great change after solution heat treating. Most of the pearlite colonies disappeared but significant grain growth was not observed.

Figure 1 shows the  $\phi = 45^\circ$  sections of the CODF for the cold rolled materials. The textures can be represented by  $\{111\} \langle uvw \rangle + \{hkl\} \langle 110 \rangle$  components with peaks near A -  $\{111\} \langle 11\bar{2} \rangle$ , B -  $\{223\} \langle 1\bar{1}0 \rangle$  and C -  $\{001\} \langle 110 \rangle$ . By far the highest peaks occur for the solution treated material. One can see that component B in material S practically disappears in SA2 and SA4 but returns slightly in material SA6. The highest peak shifts from the B component, in material S, to the C component in the others. Figure 2 is a plot of function height versus initial condition for the rolled materials. Here, the cold rolling texture of the AR material was included for comparison. Clearly the  $\{111\} \langle uvw \rangle$  components pass through a maximum for the S material and through a minimum for the SA2, increasing again for the SA6 condition, the C component remains nearly constant.

The CODF for the annealed materials can be seen in figure 3. Again the textures can be represented by the two partial fibers mentioned above but, now, the peaks occur near components A, C, D -  $\{111\} \langle 1\bar{1}0 \rangle$  and E -  $\{113\} \langle 1\bar{1}0 \rangle$ . The highest peaks, associated with the A component, occur again in the S material, where the C component has the smallest value. Figure 4 shows the function height versus initial condition for the annealed materials. Again, the maximum occurs near  $\{111\} \langle uvw \rangle$  for the solution treated material and the minimum for materials aged at 473K ( $200^\circ\text{C}$ ).

## DISCUSSION

From the results it is clear that the presence of carbide particles in the matrix affects the cold rolling texture development in sheet steels. In figure 2 it is also clear that the  $\{001\} \langle uvw \rangle$  components are much less sensitive than  $\{111\} \langle uvw \rangle$  components. In fact the latter increase considerably in the absence of carbides, as in material S, and is deeply reduced in the aged materials, while the  $\{001\} \langle uvw \rangle$  components remain practically constant. At 473K ( $200^\circ\text{C}$ ), orthorhombic cementite precipitates as platelets on  $\{110\}_\alpha$  planes in  $\langle 111 \rangle_\alpha$  directions<sup>9</sup>. At this

temperature, at peak hardness, it must be a fine and well distributed precipitation, capable of strongly interfering with the dislocation motion on the pencil glide  $\{hk\ell\}$   $\langle 111 \rangle$  slip systems. For some reason the additional displacements<sup>α</sup> resulting from the dislocation-particle interference seem to affect the rotation path of the crystals towards  $\sim \{111\}$   $\langle uvw \rangle$  end orientations more effectively than towards  $\{100\}$   $\langle 110 \rangle$ , leading to a greater randomization of the rolling texture. This in turn leads to more randomized annealing textures. As the particles coarsen their influence decreases and the material returns to a situation similar to the AR condition, as can be seen for materials SA4 and SA6 in figure 2.

The analysis of the recrystallization textures is more complicated since both nucleation and grain growth are involved. As pointed out somewhere else<sup>10</sup> the particles tend to redistribute the stored energy of cold work throughout the crystal orientations leading to a more distribution of orientations of the recrystallization nuclei. Their growth is again affected by the particles, the more so the finer their distribution, contributing to additional competition and texture randomization. This general effect can be seen in figures 3 and 4. There it can also be seen that the strongest annealing texture occurred in the solution treated material contrary to other author's<sup>3</sup> reports about the detrimental effect of dissolved carbon in rapidly annealed steel sheets.

The extreme microstructural conditions used in the present work point to a general influence of particles on both rolling and recrystallization textures, underlining what some researchers had already indicated:<sup>3,4</sup> a clean ferrite matrix with a few spread out coarse particles yields high R-values in continuous annealing.

## CONCLUSIONS

- 1 - The general influence of a fine carbide distribution in fast annealed sheet steel is to decrease the  $\sim \{111\}$   $\langle uvw \rangle$  components of both the cold rolling and the annealing textures.
- 2 - The solution treated material yields the highest peaks in the  $\sim \{111\}$   $\langle uvw \rangle$  components for both the rolling and the annealing textures.

**ACKNOWLEDGEMENTS**

The authors thank CNPq and IME for material and financial support.

**REFERENCES**

- 1 - R.L. Whileley and D.E. Wise, Flat Rolled Prod. III, Ed. A.E. Earhart, Chicago, 1962, p. 47.
- 2 - D.J. Goodwill, PhD thesis, Univ. of Cambridge, England, 1973.
- 3 - W.B. Hutchinson and K. Ushioda, Proceedings of 7th ICOTOM, Noordwijkerhout, The Netherlands, (1984), 400.
- 4 - W.B. Hutchinson and K. Ushioda, Scand. J. Met., 13(1984), 269.
- 5 - S. Ono, P. Delaneau and B. Thomas, Proceedings of 7th ICOTOM, Noordwijkerhout, The Netherlands, (1984), 359.
- 6 - I.L. Dillamore, W.B. Hutchinson and D.L. Morris, Proc. Effect of Second-Phase Particles on Mechanical Properties of Steels, The Iron and Steels Institute, London, (1971), 190.
- 7 - A.S. Magnabosco, M.Sci Thesis IME, Rio de Janeiro, 1986,
- 8 - W.F. Hosford and R.H. Zeisloft, Met. Trans., 3(1972),113.
- 9 - Steels, Microstructure and Properties, R.W.K. Heneycombe, Edward Arnold, 1981.

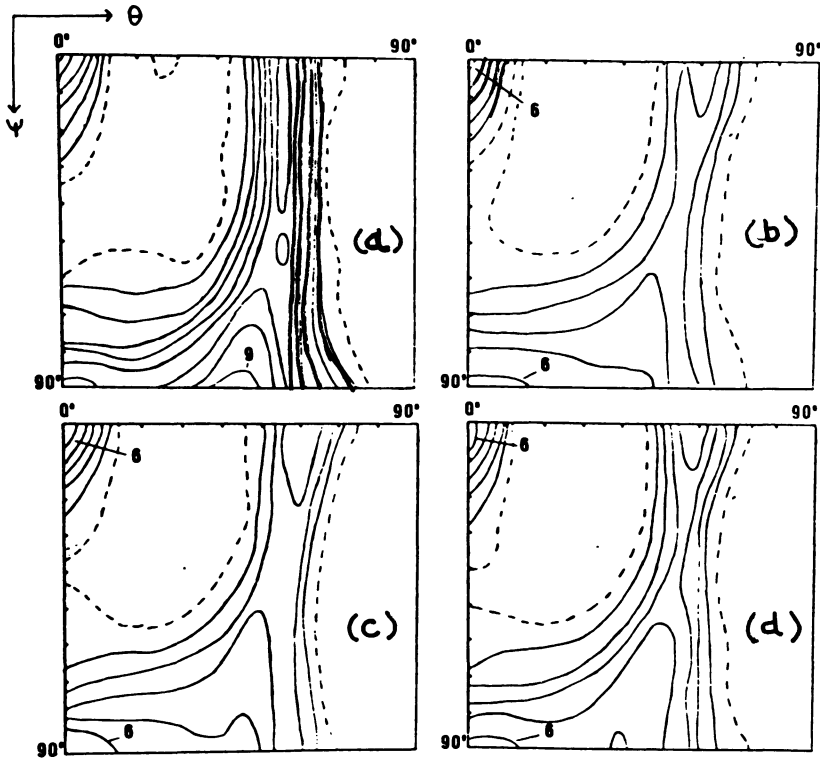


Figure 1  $\phi = 45^\circ$  sections of (a) S (b) SA2 (c) SA4 and (d) SA6 materials

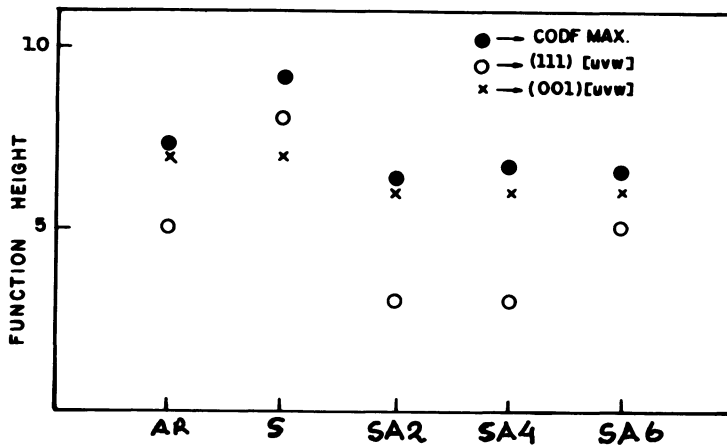


Figure 2 Function height versus previous condition for cold rolled materials

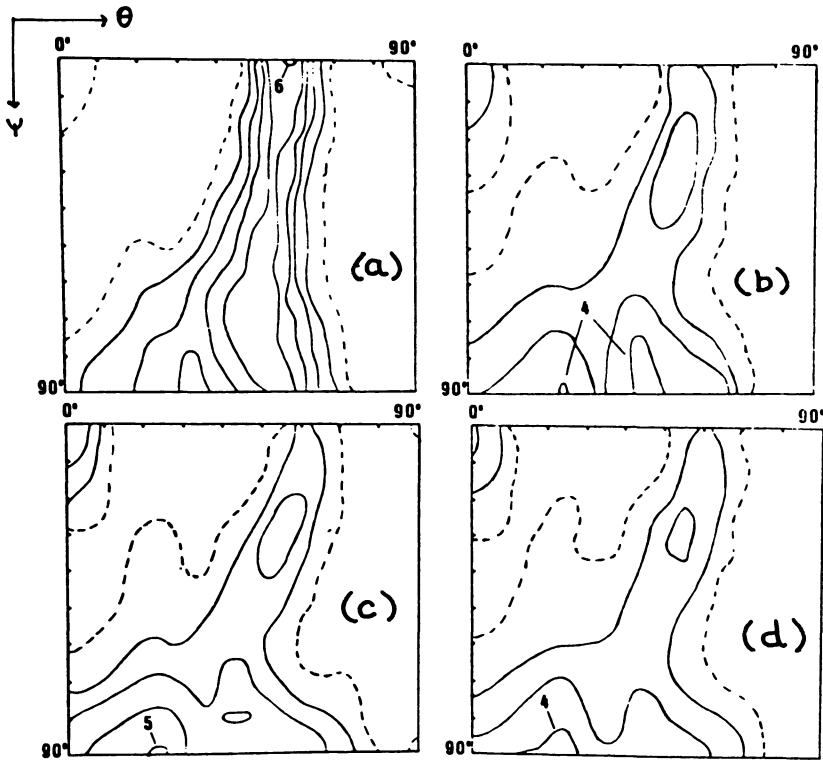


Figure 3  $\phi = 45^\circ$  sections of (a) S (b) SA2 (c) SA4 and (d) SA6 annealing textures

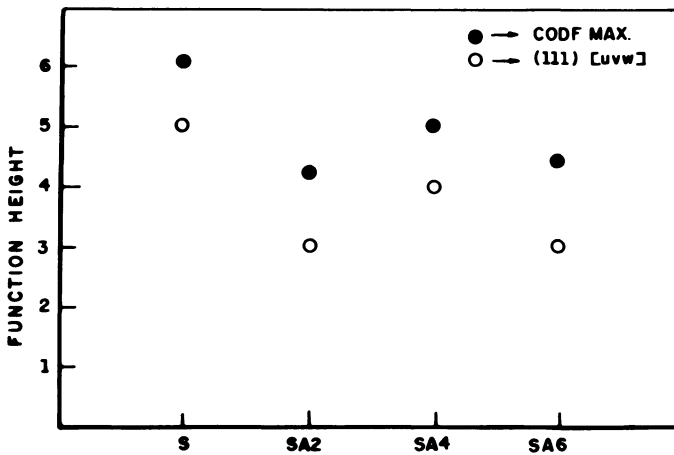


Figure 4 Function height versus previous condition for annealed materials